Possibilities and limitations of using iPhone 13 Pro with built-in LiDAR sensor in cave research – on the example of paleoflow analysis in Mylna Cave (Western Tatra Mts, Poland)

Przemysław Pluta[1], Dawid Siemek[2]

[1] Faculty of Natural Sciences, University of Silesia in Katowice, Sosnowiec, Poland, e-mail: przemyslaw.pluta@o365.us.edu.pl
[2] Institute of Geography and Spatial Management, Jagiellonian University in Kraków, Kraków, Poland,

Abstract: The study tested the capabilities of the Apple iPhone 13 Pro device using two measurement techniques, LiDAR (Light Detection and Ranging) and SfM (Structure from Motion), in a cave environment by measuring scallops in Mylna Cave in Western Tatra Mountains. The tested device provides an interesting and inexpensive alternative for cave research using TLS (Terrestrial Land Scanner) type scanners or more expensive MLS (Mobile Laser Scanning) type scanners. The study used a dedicated 3D Scanner App™ application to create two terrain models: LiDAR and SfM. A comparative analysis of the models shows that the SfM model is characterised by greater detail. The results obtained for this model indicate that the scallops measured in Wielki Chodnik passage of Mylna Cave belong to at least two different generations of forms. In the LiDAR method case, the obtained models' resolution was not precise enough to identify small (<3 cm) scallops. For three LiDAR models, the average length of scallops was 10.32 cm; for three SfM models, it was 5.16 cm. The length of scallops obtained from models allowed for calculating paleoflow velocity and, thus, the flow rate. The average velocity value for LiDAR models was 28.98 cm s⁻¹, and for SfM models – 48.10 cm s⁻¹ and the average flow rate obtained from SfM data was 1.93 m³ s⁻¹. It corresponds well with the today-observed Kościeliski Potok flow rate of 1.7 m³ s⁻¹ according to the 1966–2000 period (Baścik et al. 2014). On the contrary, the average paleoflow rate obtained from the LiDAR model, which is 0.94 m³ s⁻¹, does not match the contemporary flow rate. Based on the asymmetry of scallops, the paleoflow direction was determined. It is consistent with the current direction of the Kościeliski Potok flow. The spatial imaging techniques used with iPhone 13 Pro differ regarding the DEM creation method and model details. It is influenced by parameters related to lighting, distance, scanned surface character and microclimatic conditions of the cave.

Key words: DEM, LiDAR, SfM, iPhone 13 Pro, paleoflow, Mylna Cave, Tatra Mts

Introduction

Laser scanning has become a standard method of documentation and 3D modelling in caves in the last decade (Gallay et al. 2016, Pukanská et al. 2020, Cossoa et al. 2022). LiDAR (Light Detection and Ranging) is a measuring technique using a laser beam that returns to the device after reflection, and the distance is measured based on a time interval. An example of this type of device is TLS (Terrestrial Laser Scanning), whose construction allows sequential scanning of the environment in horizontal and vertical directions (Dabove et al. 2019, Konsolaki et al. 2020). TLS has been used in speleological research

(Gallay et al. 2016, Konsolaki et al. 2020). However, its use is relatively expensive and logistically challenging, especially in unfavourable cave conditions (Eitel et al. 2013, Buchroithner 2015). An interesting alternative to TLS seems to be MLS (mobile laser scanning), which allows the collection of field data in a handy way. However, using this device depends on the cost of software or the size of the analysed area and can often exceed tens of thousands of pounds (James, Quinton 2014, Bauwens 2016).

In 2020, Apple Inc. launched a series of iPad Pro and iPhone Pro devices with a built-in LiDAR sensor. Mobile devices equipped with this sensor can be widely used in earth sciences due to the relatively

low cost of the device, its easy operation or the increasing number of users who can contribute to the development of science (Luetzenburg et al. 2021). In addition, using free applications, pre-processing and exporting data from the device can occur intuitively.

The possibilities of using the tool in environmental research have recently been presented in several papers (Luetzenburg et al. 2021, Mikita et al. 2022, Tatsumi et al. 2022). It is noteworthy that the device has already been utilised in the context of cave studies aimed at documenting graffiti in Indonesia (Kartini et al. 2022). However, research focused on cave morphology and forms has not been conducted. Filling this gap in this article we aimed at testing and evaluating the LiDAR tool in iPhone Pro series smartphones for corrosive forms called scallops. The study presents the results of research carried out in Mylna Cave in Western Tatras (Poland) using the iPhone 13 Pro device. The device is at the disposal of the Institute of Earth Sciences of the University of Silesia in Katowice. The main goal of the study was to assess the functionality and evaluate the limitations of the use of iPhone Pro with LiDAR sensor in cave conditions and compare numerical models obtained using two techniques: LiDAR and Structure from Motion (SfM). In addition, the aim was also to determine the potential direction and velocity of paleoflow in Mylna Cave based on scallops length and asymmetry measurements.

Methods

Fieldwork

The research was conducted in Mylna Cave, open to tourists and characterised by various passage relief. Mylna Cave together with Obłazkowa Cave and Raptawicka Cave is part of Pawlikowski Cave System, located on the western slopes of Kościeliska Valley in Western Tatras (Fig. 1). The total length of the passages of Pawlikowski Cave System is 2404 m, of which 1630 m belongs to Mylna Cave. This cave developed in the massive Upper Jurassic – Lower Cretaceous limestones (Kotański 1959, Lefeld et al. 1985). The cave was developed on the system of joints and bedding planes modelled by the underground flows of the former Kościeliski Potok stream, which flowed at this altitude in the pre-Pleistocene period (Rudnicki 1958, 1967). In the final section of the cave, in the so-called Wielki Chodnik passage, well-developed and preserved scallops occur. They are remnants of paleoflow in the phreatic and epiphreatic zones of the karst system.

Scallops are among the most characteristic corrosive forms on the walls of karst caves. At the same time, they belong to the group of diagnostic forms that allow us to infer the origin of cave passages. Scallops are asymmetrical depressions formed due to
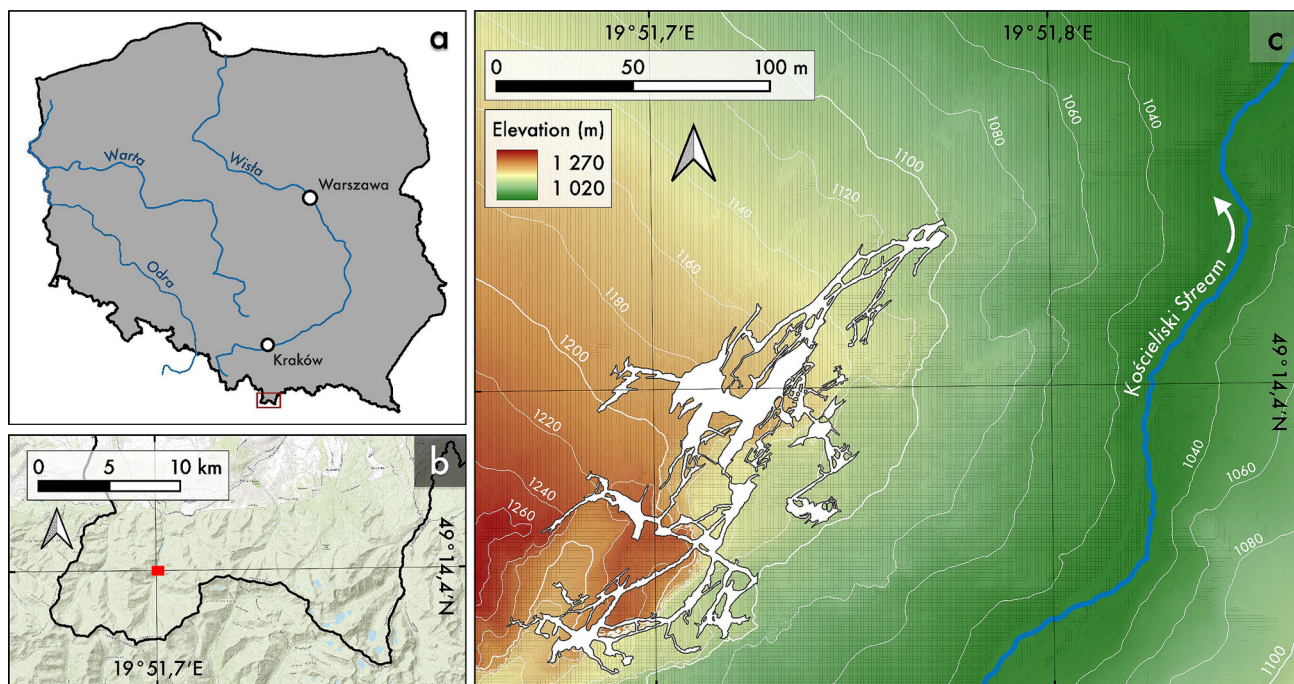

Fig. 1. Study area: a – location of the Tatra Mts. in Poland; b – location of Raptawicka Turnia Massiv in Western Tatras (based on ESRI World Topo); c – Pawlikowski Cave System and Kościeliski Stream against the background of hypsometric map and DEM (based on spatial data available on GUGiK 2023)
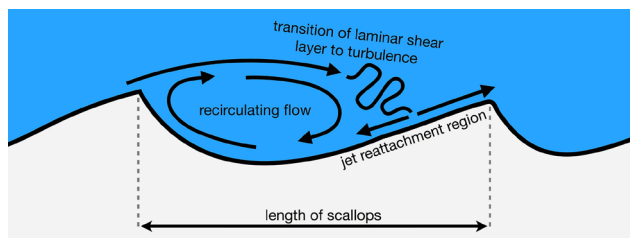
Fig. 2. Cross-section and specificity of flow near the scallop based on Curl (1974)

dissolving rock walls under the influence of turbulent flow (Fig. 2) (Slabe 1995, Palmer 2007, De Waele, Gutiérrez 2022). They are used to determine the conditions of former flow in cave passages that are currently dry. Scallops reach sizes from about 0.5 cm to even 2 metres. The asymmetry of scallops indicates the direction of flow that either formed the cave passage or modelled it at a later time, such as during the flow of water from melting glaciers. This was pointed out by Bretz (1942) and Coleman (1949). In turn, by determining the average length of scallops (it is assumed that based on measurements of at least 30 scallops), it is possible to determine the speed of the youngest and most intense flow in the cave passage (Palmer 2007, De Waele, Gutiérez 2022). The relationship between the size of scallops and the speed of water flow in the passage was experimentally determined by Rudnicki (1960), and world literature included the results of Curl (1966, 1974) and Blumberg and Curl (1974). Three measuring stations located in the final section of Mylna Cave were selected for the study – Wielki Chodnik passage. Site 1 is locat-

ed near the siphon, down the passage. Sites 2 and 3 are located in the central part of the passage, on its opposite wall, which is important when interpreting specific directions of the paleoflow (Figs 3, 4). The distance between the furthest stations was about 25 meters. In order to make georeferences, nine checkpoints (modelling clay balls) with a diameter of about 1 cm were placed on each of the sites, in a spacing of 50 cm, thus creating a square with an area of approx. 1 m² (Fig. 4b).

During the scan, the iPhone was supported manually, and the profiles were illuminated with neutral, diffused light directed towards the scanned surface (Fig. 4b). Armytek Wizard C2 Pro Max flashlight with white light was used for lighting. Trial scans have been performed for each site to determine the appropriate way to drive the device and set lighting conditions. Scanning was processed sequentially while maintaining a distance of about 30 cm from the scanned surface (Figs 4a, b).

During fieldwork, the Apple iPhone 13 Pro device with a built-in LiDAR scanner was used. The scanner uses its triangulation grid (Luetzenburg et al. 2021) based on the software platform Apple Inc. ARKit, which means it can be used without a connection to an external GNSS system. The device manufacturer does not provide official information about the scanner specifications. The Laan Labs application 3D Scanner App™ version 1.9.8 which capabilities have also been tested in other environmental works (Luetzenburg et al. 2021, Mokroš et al. 2021, Gollob et al. 2021, Mikita et al. 2022) was used.
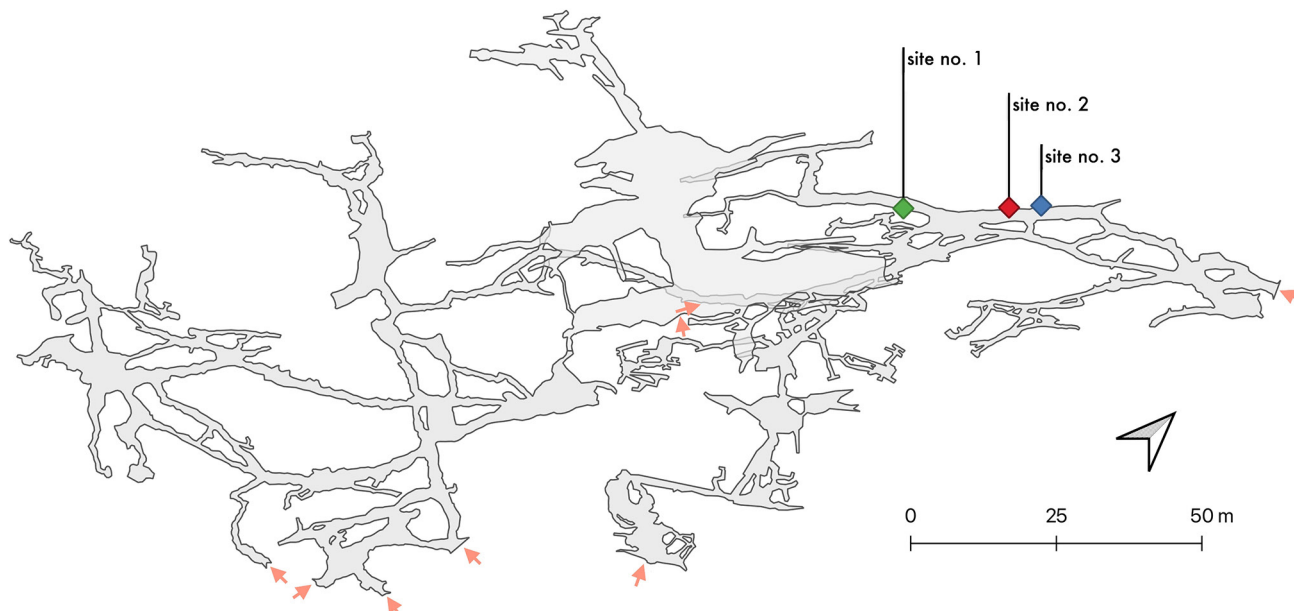

Fig. 3. Location of the examined sites in Wielki Chodnik passage in Pawlikowski Cave System; cave plan acc. to Filar, Parczewski (2015)
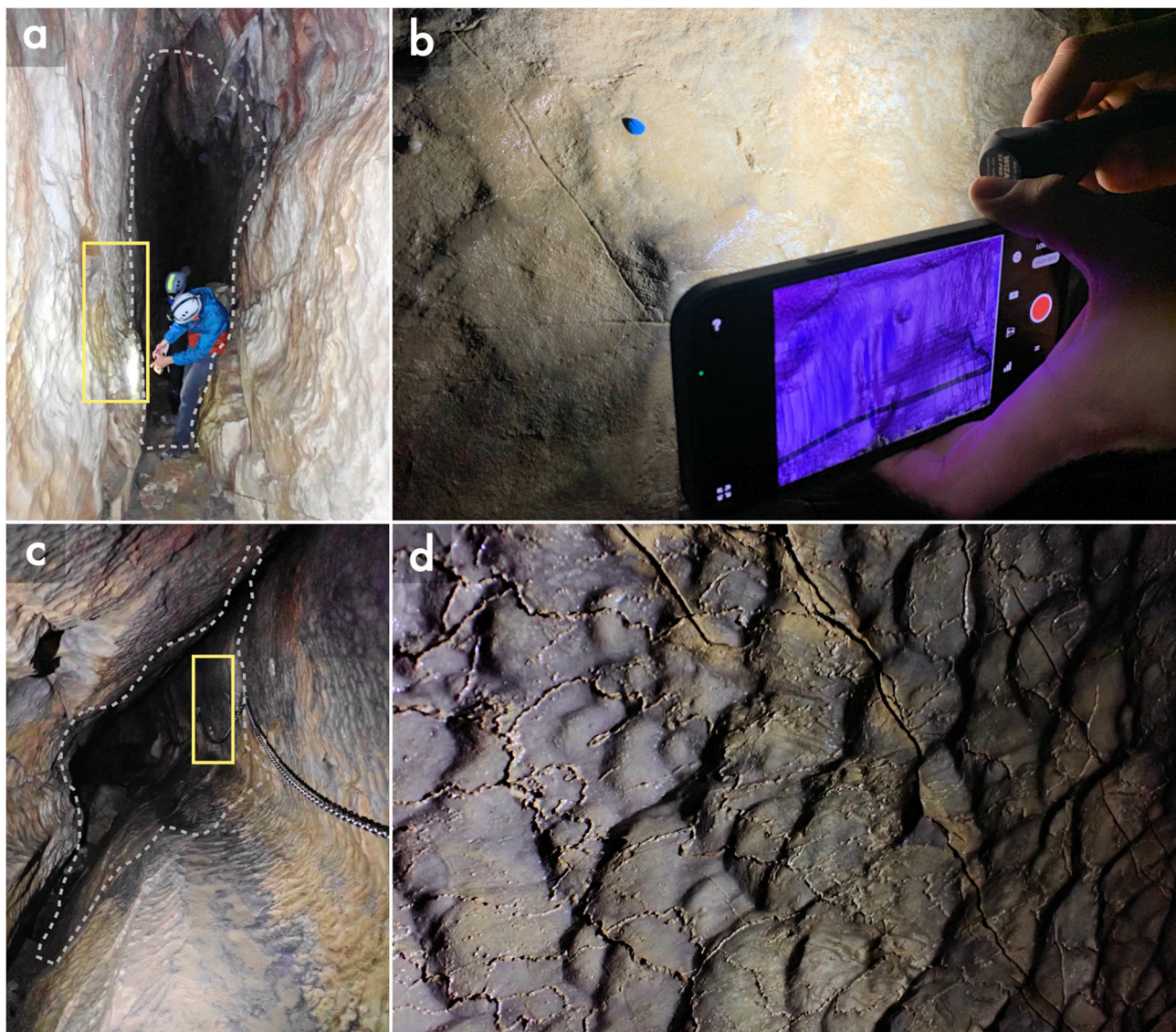
Fig. 4. Walls of Wielki Chodnik passage: a – site no. 1, b – method for marking the checkpoints of measuring sites and lighting and guiding the iPhone 13 Pro during scanning site no. 1, c – site no. 2 (cross-sections of the passage are marked by a dashed line and the examined parts by yellow rectangles), d – scallops near site no 3. (Photo: A. Tyc, P. Pluta)

Processing data

A point cloud with an area of about 2 m² for each station was obtained from scanned profiles. Based on the exported data, two 3D models were created for each site – LiDAR models (exported in LAS format from the application) and SfM models, based on photos taken at 1.9 fps s⁻¹. The SfM models in OBJ format were created using the 3d Scanner App™ program available on macOS version 1.1.1. Then, the models were converted to a standard LAS model in CloudCompare version v.2.12.1. Georeference were given to SfM models by matching with proper size LiDAR models. Models were matched by selecting at least four equivalent pairs of checkpoints. Based on the differences in distance between checkpoints

for the obtained models in QGIS software version 3.22.7 (Białowieża), the average fit error was determined at ~0.05m. Point clouds were then exported from CloudCompare to the form of a text file – ASCII cloud. While maintaining the X, Y, and Z point coordinates, the processed data was loaded into QGIS

Table 1. Comparison of area fields and point density for LiDAR and SfM models

Site	Site area	Point cloud density	
		iPhone LiDAR model	SfM model
	[m²]	[pts m⁻²]	
no. 1	1.76	32,105.35	436,880.06
no. 2	1.36	33,153.25	323,557.32
no. 3	2.20	33,883.71	168,807.52

software. Models were trimmed, taking into account the occurrence of checkpoints and eliminating distorted edges, giving models the shape of rectangular surfaces with different surfaces (Table 1). The loaded point layer was subjected to the Triangulated Irregular Network (TIN) interpolation process to obtain the Digital Elevation Model (DEM).

Determination of the paleoflow direction

The direction of paleoflow has been determined in two ways. The first method was semi-automatic direction measurement based on exposure and slope indexes. First, the slope model was cut to 20° (SfM model) and 10° (LiDAR model). The basis for this was visual observations – it was noticed that the steepest areas on the profiles correspond to erosion undercuts (Fig. 2). Then, the exposure model obtained in this way was trimmed into the slope model, which was then reclassified, dividing it into four classes, corresponding to opposite directions of the world: N–S, NE–SW, E–W and SE–NW. Due to the use of the exposure model for the vertical or almost vertical wall of the cave, abbreviations of the terms U – up, D – down, L – left and R – right were used instead of marking the directions of the world. This gave appropriate markings of opposite directions on the cave wall: U–D, UR–DL, R–L and DR–UL. Each class thus received a range of 90°. Subsequently, the obtained classes were subjected to polygonization and then aggregation. The final stage was to calculate the percentage share of a given class in the entire analysed area, i.e. the exposure model cut to the slope model. This way, a potential paleoflow vector was obtained, but without a specific direction. This method was complemented by a manual examination of scallops asymmetry when determining the scallops length. Hillshade (Fig. 5), exposure and slope indexes generated from DEM were used to draw lines consistent with asymmetry. Then, for the selected lines, the direction was specified, which was compiled for each site, giving its average value.

Calculation of paleoflow velocity and flow rate

Paleoflow velocity (u') was calculated using the Curl equation (1974). The lengths of scallops were used to carry out the calculations, which were used to output the average Sauter (L_{32}). Their length was measured manually on DEM using the Profile Tool plugin version 4.2.2 in QGIS. To calculate kinematic viscosity (μ) and water density (ρ), a water temperature of 4°C was assumed. Subsequent values, i.e. Reynolds number (Re*) and fractional factor (B_L) were adopted,
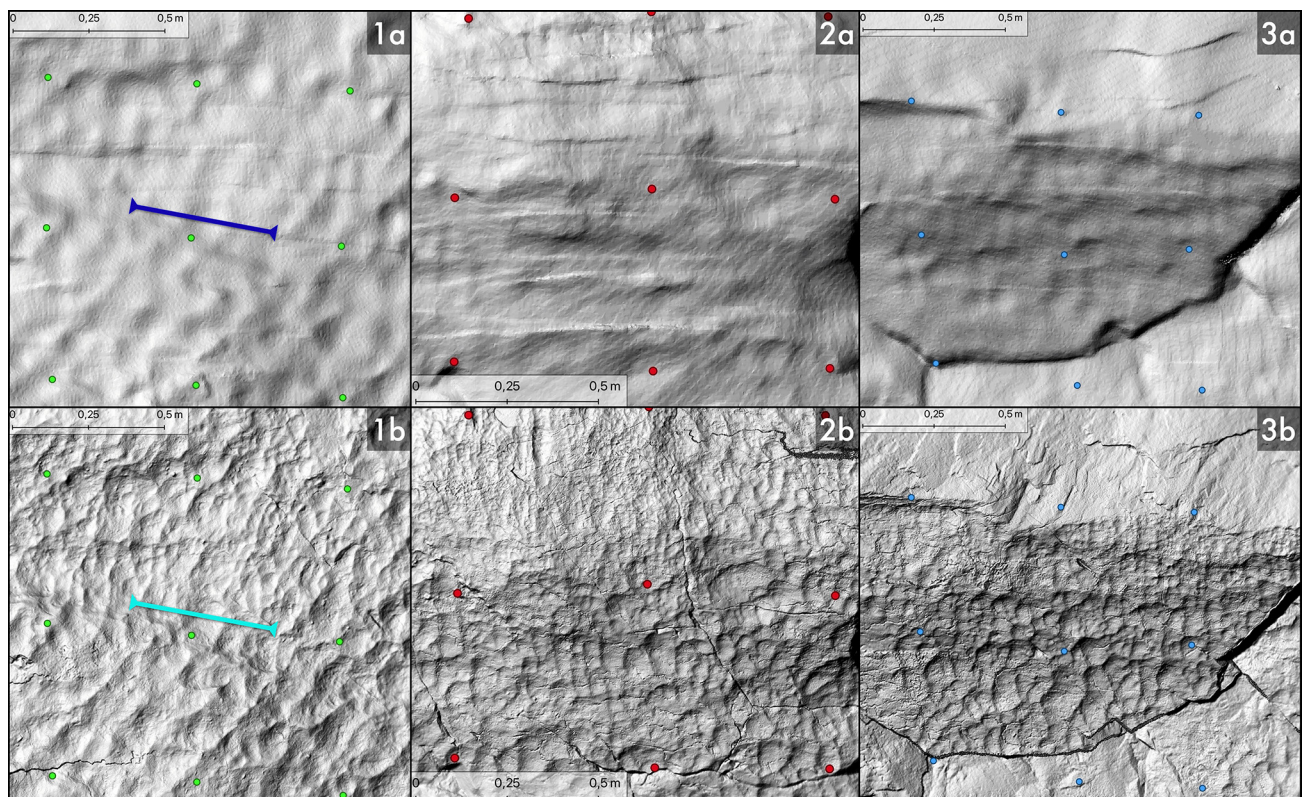

Fig. 5. Hillshade index generated for iPhone LiDAR models (1–3a) and SfM models (1–3b). Checkpoints are marked with colourful dots. The navy blue and turquoise lines refer to the profile cross-section presented in Fig. 6

according to literature (Blumberg, Curl 1974) – they were 2200 and 9.4, respectively. The analysis considers two cross-sections of the cave passage: rectangular (Fig. 4a) and round (Fig. 4c), using separate equations-presented below (Blumberg, Curl 1974):
– the mean velocity u' (cm s^{-1}) for a circular conduit

$$u' = \frac{\mu}{\rho L_{32}} Re^* \left[2.5 \left(\ln \frac{D}{2L_{32}} - 1 \right) + B_L \right.$$

– the mean velocity u' (cm s^{-1}) for a rectangle conduit

$$u' = \frac{\mu}{\rho L_{32}} Re^* \left[2.5 \left(\ln \frac{D}{2L_{32}} - 1.5 \right) + B_L \right.$$

Knowing the speed of water flow and the approximate cross-sectional area of the passages, the water flow rate was calculated according to the formula:

$$Q = v \times A$$

where:
– v – flow velocity (cm s^{-1})
– A – cross-sectional vector area (m^2).

Results

Length of scallops

The obtained DEM was used to determine the length of the scallops. For this purpose, the measurement was made manually, marking on all six 3D models the length of individual scallops, guided by the asymmetry of forms and looking for the longest possible diagonal. For the LiDAR model, 50 objects were designated, and for the SfM model, 200 objects were for measurement. The SfM model made it possible to recognise scallops of smaller size, which is associated with greater detail of the created models (Table 2;

Figs 5, 6). The average length of scallops calculated on the SfM models was 5.16 cm, and the most significant percentage was observed in the range of about 3–5 cm. The average length of the LiDAR models was 10.32 cm, and the percentage of scallops in the range of about 7–9 cm constituted a representative majority for this model. The smallest forms that could be recognised on the LiDAR model were usually no less than 3 cm long (Fig. 7).

Paleoflow direction

The obtained values of the paleoflow direction vary depending on the analysed position and the accuracy of DEM. From LiDAR models, only the direction at site 1 can be considered relatively correct, while directions at sites 2 and 3 do entirely not reflect the character of paleoflow. In the case of surfaces scanned in a vertical plane, the wind rose had to be adapted to the appropriate spatial orientation representing the directions relative to the observer (up – U, down – D, left – L, right – R) (Fig. 8). The percentage of directions at site 1 is respectively: 43 % (U–D), 23% (UR–DL), 20% (DR–UL) and 14% (R–L) (Table 3). Much greater accuracy, and thus more reliable results, are characterised by values obtained for SfM models. Sites 1 and 3 are dominated by U–D direction (32% and 62%, respectively), and at site 2 DR–UL direction (33%). The percentage share of UR–DL direction ranges from 24% (site 1) to 32% (site 3) (Table 3). At all sites, the share of the R–L direction is the smallest and ranges from about 19% (site 1) to 1% (site 3). At site 3, the share of DR–UL direction is also the smallest and amounts to less than 5%. The average value of the scallops azimuth (black arrows in Fig. 8) is about 90° for sites 2 and 3 (both LiDAR and SfM models), while at site 1 it is 282° (LiDAR model) and 286° (SfM model). The best correlation between the results of both methods used is seen at site 1. This relationship is less visible at site 2, while at site 3 the results are entirely different.
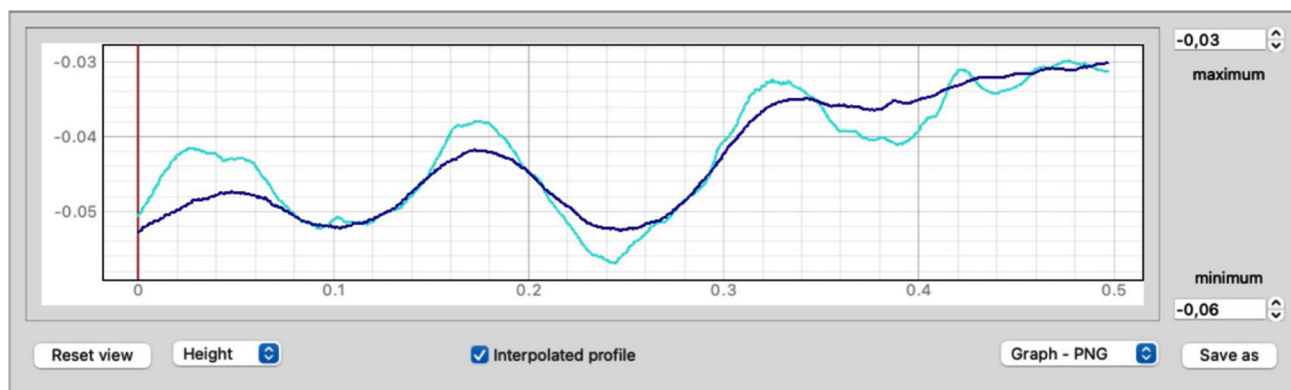

Fig. 6. Profile tool plugin window view showing a cross-section graph for the SfM model (turquoise colour) and iPhone LiDAR model (navy blue colour) of the selected section in site no. 1 marked in Fig. 5

Table 2. Parameters of the measured scallops and calculated paleoflows

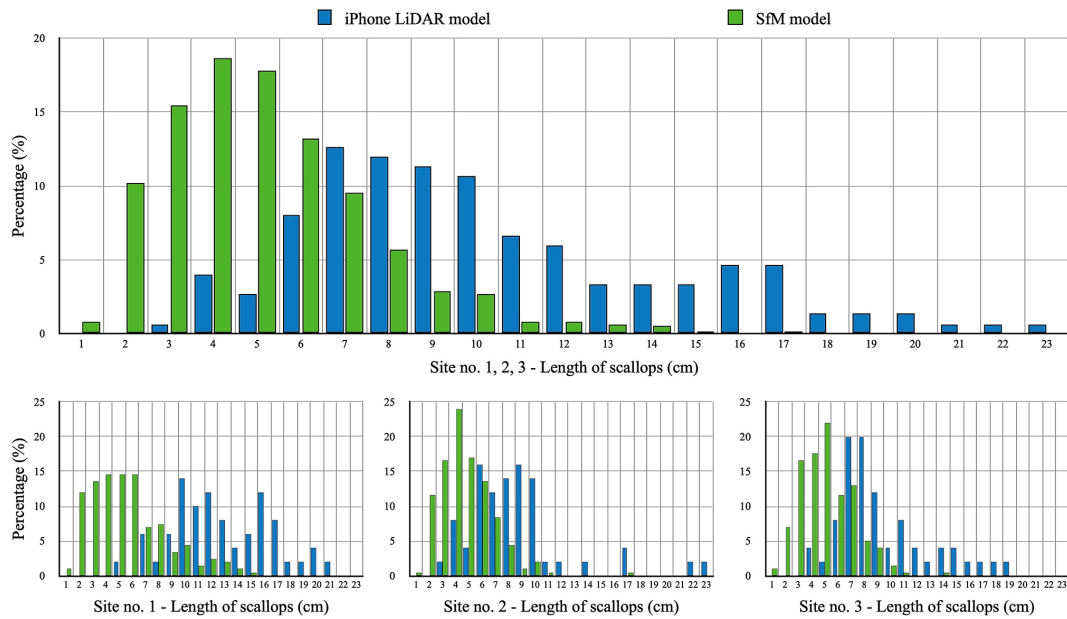| Site	Model	Number of measured scallops	Minimum and maximum length of scallops	Average length of scallops	Average paleoflow speed	Paleoflow discharge	Paleoflow direction
		[–]	[cm]		[cm s⁻¹]	[m³ s⁻¹]	
no. 1	iPhone LiDAR	50	5.27–20.79	12.90	20.15	0.71	NE
	SfM	200	1.04–15.32	5.67	40.23	1.41	NE
no. 2	iPhone LiDAR	50	3.32–22.78	8.61	32.08	1.01	NE
	SfM	200	1.34–17.44	4.75	69.37	2.18	NE
no. 3	iPhone LiDAR	50	4.23–18.60	9.44	34.71	1.09	NE
	SfM	200	1.21–14.30	5.06	69.94	2.20	NE

Fig. 7. The relationship between the number of measured scallops (expressed as a percentage) and their length
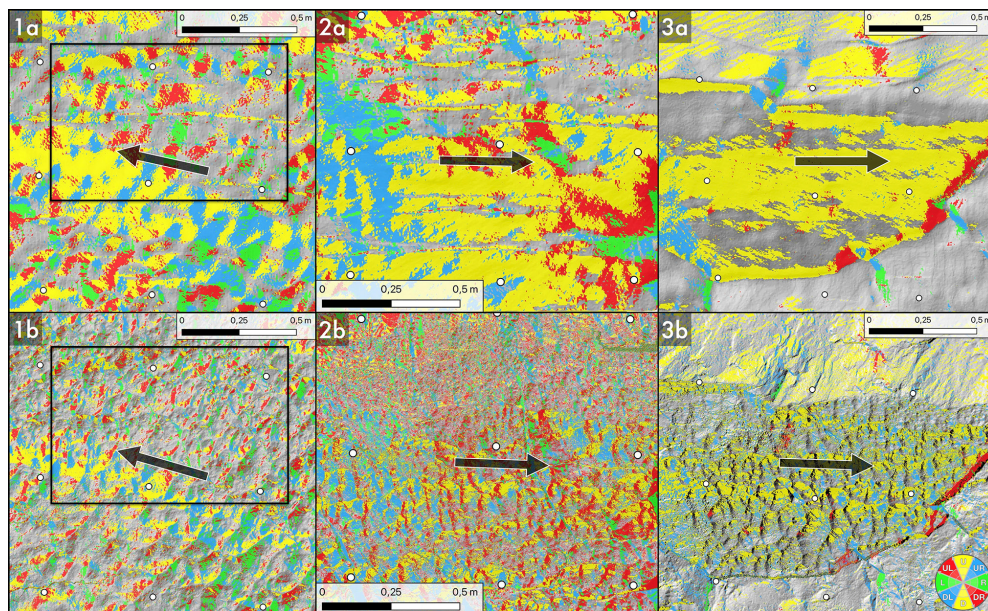

Fig. 8. Fig. 8. Exposure index above 10 degrees for iPhone LiDAR models (upper segment) and above 20 degrees for SfM models (lower segment) with superimposed hillshade index for 3 iPhone LiDAR models (1a, 2a, 3a for site no. 1, 2, 3) and 3 SfM models respectively (1b, 2b, 3b for site no. 1, 2, 3). Black arrows show the potential flow direction based on the average azimuth value from the scallops' cross-sections. The area delineated by the black boundary indicates the region in Fig. 9

Table 3. Percentage of paleoflow directions calculated for LiDAR and SfM models based on exposure index. The values indicate the share of a given direction in the entire surface inclined above 20 degrees for the SfM model and above 10 degrees for the LiDAR model (U – up, D – down, L – left, R – right)

Directions	Site no. 1		Site no. 2		Site no. 3	
	LiDAR model	SfM model	LiDAR model	SfM model	LiDAR model	SfM model
	[%]					
U–D	43.0	32.0	54.0	29.9	83.0	62.4
UR–DL	23.4	24.0	21.0	25.3	9.0	31.8
R–L	14.0	18.7	8.0	11.5	2.0	1.2
DR–UL	19.6	25.3	17.0	33.3	6.0	4.7

Paleoflow velocity

Based on the Curl equation (1974) using the length of the scallops for the three selected measuring sites in Wielki Chodnik passage of Mylna Cave, the velocity of the paleoflow was calculated (Table 2). The estimated velocity for the LiDAR model located near the siphon (site 1) was 20.2 cm s^{-1}. Paleoflow velocity for successive sites increased with moving deep into the passage in a northeast direction to the exit, respectively: 32.1 cm s^{-1} for site 2 and 34.7 cm s^{-1} for site 3. A similar distribution of velocity proportions characterises paleoflow estimated based on the SfM model. However, the values are about twice as high as the iPhone LiDAR model. The lowest paleoflow velocity was calculated for site 1 (40.2 cm s^{-1}), and for site 2 (69.4 cm s^{-1}). For the sites 3 and 5 m away, a similar one were obtained (69.9 cm s^{-1}).

Discussions

Differences in the models resolution

The results of scanning three test surfaces on the walls of Wielki Chodnik passage in Mylna Cave in Tatra Mountains using the iPhone 13 Pro allow for a comparative analysis of the techniques used to create DEM. The essential element distinguishing LiDAR models from those obtained using SfM is the level of their detail, resulting from the density of the point cloud for a single model, i.e. the resolution of the raster (Table 1).

The density of the point cloud for LiDAR models ranges from 32,105 (site 1) to 33,884 (site 3) pts m^2 (Table 1). On average, for LiDAR models, an image of 33,054 pts m^2 was obtained. In turn, SfM models are characterised by a much higher density of the point cloud. At the same time, this density varied wildly between models and ranges between 168 808 and 436 880 pts, with a distribution opposite to density for LiDAR models (Table 1; Fig. 9). Different resolution of models affects the efficiency of measuring individual scallops, and consequently velocity and paleoflow rate in the studied passage of the cave. The lower resolution of LiDAR models influences the ability to identify smaller scallops in the case of models obtained for Mylna Cave smaller than 3 cm (Figs 5, 7). At the same time, on these models, the largest number of identified forms is in the range of 6–12 cm (on average 10.32 cm) and even 10–17 cm at site 1. Higher resolution of models obtained using SfM techniques allows identification and measuring of much smaller scallops. The percentage distribution of the measured
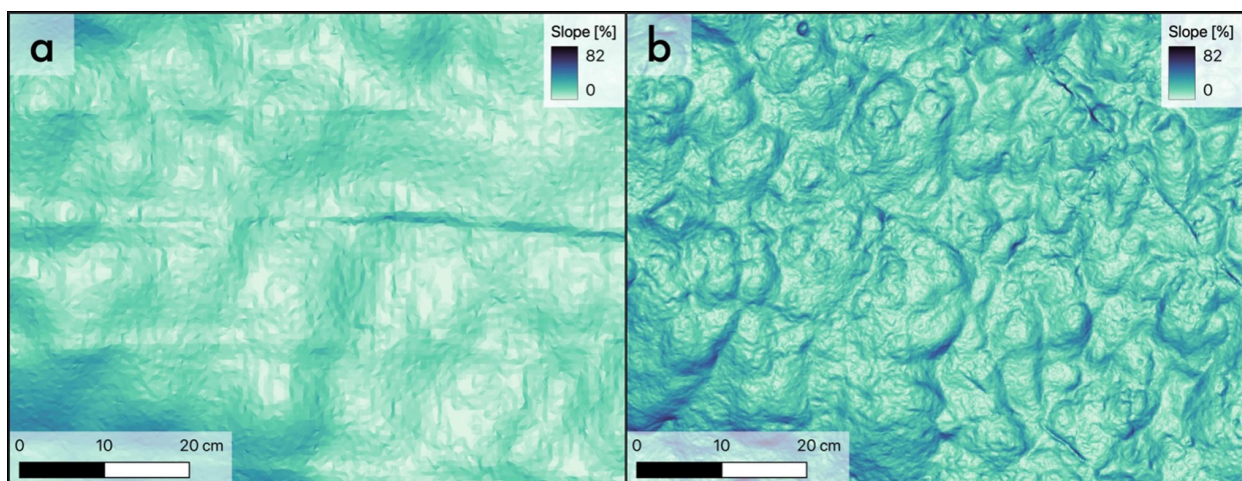

Fig. 9. Slope index for the same fragment of the iPhone LiDAR model model (a) and the SfM models (b), highlighted in black colour in Fig 8

forms' length indicates the possibility of identifying scallops up to 1 cm long, with the range of the most significant number of identified forms from 2 to 8 cm (on average 5.16 cm; Figs 5, 7). Differences in scallop length result directly from the model's detail. These, in turn, are associated with factors whose control is often difficult or even impossible during measurement, such as appropriate lighting or the method of conducting the device during scanning.

Comparative analysis of LiDAR and SfM numerical models shows that depending on the techniques used, we can expect different analytical potentials, with the SfM model enabling the identification of smaller forms. Therefore, it is suitable for calculating the paleoflow parameters in the cave. However, it seems that, at the moment, the best option is to use both measurement techniques. It should be emphasised that data for numerical models developed by both methods are obtained during one scanning process in the cave and created using the same application dedicated to Apple devices. A significant advantage of the LiDAR sensor is the very principle of operation of the scanner, which does not use visible light. This can be an advantage in the situation of scanning in worse lighting conditions or the case of slightly larger objects in caves. What is more, the handiness and compactness of the iPhone 13 Pro can be conducive to mapping hard-to-reach cave parts. The universality and price of the device will probably contribute to increased interest among users and continuous improvement of both the sensors used and dedicated applications for scanning and creating models.

The method of calculating the length of scallops presented in this work seems a good alternative to *in situ* research, especially in the deeper parts of caves. Nevertheless, manual measurement of scallops length on the obtained numerical model is burdened with a subjective approach and depends on the researcher's experience. This speaks for further search for solutions to automatically measure the surface and length of scallops based on the obtained 3D model (LiDAR or SfM techniques). So far, any attempts based mainly on calculating of DEM parameters or vector analysis have not yielded satisfactory results (Droin 2021). This problem was also not solved in this study.

Scallops length calculation

Based on 3D models from Mylna Cave, an attempt was made to determine the direction of the paleoflow semi-automatically. The results shown in Figure 8 and Table 2 allow us to conclude that this goal has only been partially achieved. It should be considered that the generated LiDAR models do not provide the possibility of reliable analysis of the direction of

paleoflow because they are characterised by too low accuracy (Fig. 9a). Also, SfM models, although they are much more accurate, do not provide indisputable background to determine the paleoflow direction without supporting methods. This can be, for example, a manual measurement of the asymmetry of scallops on generated DEM. The approach used in the analysis of the paleoflow direction, i.e. a combination of opposite directions (see methodological part of this paper), is the only visually correct option to present the nature of the paleoflow. Due to very small differences (reaching up to 0.1 mm) in the parameters of individual scallops, assigning the exposure value to a specific slope value does not make sense. It is often the case that the shape, as well as the longitudinal profile of the scallops differ from each other. Hence, the slope parameter takes different values on the distal and proximal sides, which is associated with different generations of overlapping forms and the wall structure itself. However, this last situation occurs rather rarely but when it does, smaller (younger) forms overlap the bigger one (older) (Fig. 10). These factors, as well as the construction of the passage itself and errors related to the transfer of the three-dimensional surface to the plane, can affect the high incidence of U–D direction (N–S in GIS spatial analyses) visible at each analysed site.
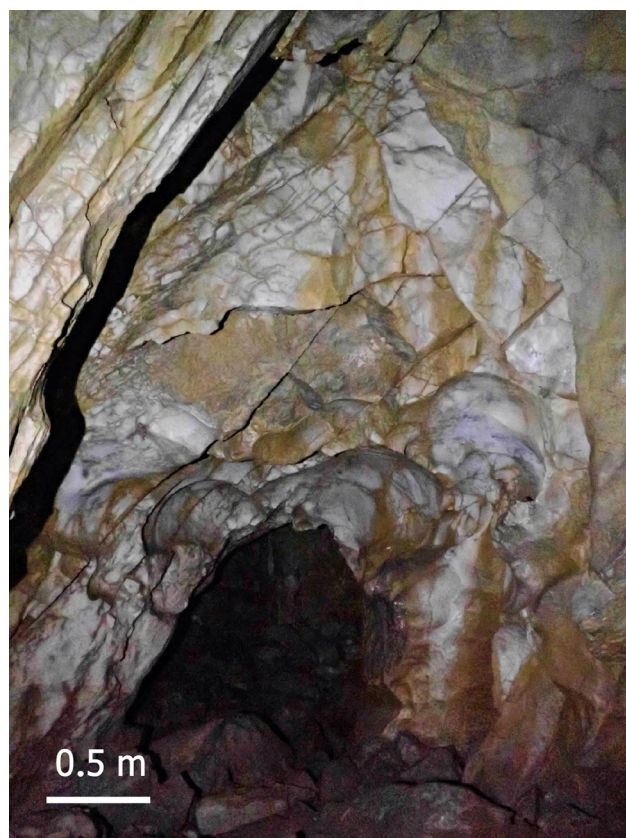

0.5 m

Fig. 10. Large scallops in the zone of the former siphon connecting the passages of Wielki Chodnik and Wysoka Szczelina in Mylna Cave (Photo by A.Tyc)

Manual measurement of scallops asymmetry is, therefore, a good complement to this type of analysis. Although it requires consistency and some discernment in the nature of the analysed profile (e.g. the presence of several generations of forms), it can be considered a good alternative to this type of activity carried out in cave conditions. Attention should be paid to faster measurement time and a much greater potential number of measured forms compared to traditional measurements. When determining the paleoflow direction, however, it is necessary to properly recognise the field combined with the analysis of the development of cave passages, as well as, at least partially, pay attention to the genesis of cave passages. This involves, for example, distinguishing real scallops from artefacts that can disrupt the results of analyses. An example of this type of artefact is the diagonal line at site 3, a significant place for mounting the chain (Figs 4c, 8 – 3b).

Paleoflow in Mylna Cave in Tatra Mountains

The obtained paleoflow velocity values for three sites located in Wielki Chodnik of Mylna Cave allowed the calculation of its flow rate (Table 2). For the analysis of the flow rate, the following cross-sectional areas of the cave passage were adopted: 3.5 m² for site 1 and 3.14 m² for site 2 and 3. The calculated paleoflow rates for SfM models are respectively: 1.41 m³ s⁻¹ for site 1, 2.18 m³ s⁻¹ for site 2 and 2.2 m³ s⁻¹ for site 3. The average paleoflow rate value for SfM models was 1.93 m³ s⁻¹, which is a similar value to the average modern flow rate in Kościeliski Potok which was 1.7 m³ s⁻¹ in 1966–2000 period (Baścik et al. 2014). The estimated paleoflow rate for LiDAR models was lower at an average of 0.94 m³ s⁻¹.

Based on the distribution of the examined sites within the cave passage and changes in the distribution of paleoflow velocity, it can be concluded that the lowest flow velocity values were recorded near the siphon, which was located several metres on SW from site 1. A relic of the siphonal flow in this part of Mylna Cave is a lowered transition passage to Wysoka Szczelina. Its walls are covered with large scallops tens of centimetres long (Fig. 10). Deeper into the cave passage towards NE (to the current artificial exit hole of the cave, Fig. 3), the velocity increased, and there were slight differences in value between the results for site 2 and 3. Regardless of the method used to create a numerical model, paleoflow velocity values have the same upward trend, consistent with the NE direction. However, it should be noted that the paleoflow velocity values calculated from LiDAR models are about twice as low as the results estimated from SfM models.

Morphology and length of cross-sections of the passage in Wielki Chodnik passage (from 1 m at

site 1 to 2 m at sites 2 and 3) allow us to compare the obtained values for research conducted in Tatra Mountains. They were preceded by relatively low, horizontally developed caves in Bystra Valley (caves: Magurska, Kalacka, Goryczkowa, Kasprowa Niżnia; Hercman, 1985; Kicińska et al. 2017). The obtained results of paleoflow velocity in Mylna Cave, which range from 40–70 cm s⁻¹ in the case of the SfM model, best correspond to the results obtained in Kalacka Cave and Kasprowa Niżnia Cave, where the velocities were calculated at about 21–77 cm s⁻¹. In Magurska and Goryczkowa caves, where generally higher values were achieved, in the range of 65–889 cm s⁻¹ (Magurska Cave) and 35–170 cm s⁻¹ (Goryczkowa Cave), only part of the results can be directly compared to the values obtained in this work. In general, in the caves of Bystra Valley, the recorded paleoflow velocities rarely exceeded 100 cm s⁻¹, which makes it possible to conclude that the paleoflow in this valley had a similar character to the paleoflow in Mylna Cave.

Summary and conclusions

The study used the iPhone 13 Pro mobile device with a built-in LiDAR sensor, which was subjected to usability analysis in the study of corrosive forms (scallops) in the cave. Testing of this device was carried out on the example of scallops in the final section of Mylna Cave, Wielki Chodnik passage, in Tatra Mountains. Three sites (profiles) with an area of about 1 m² designated on the cave walls were scanned, and then numerical models were created based on techniques – iPhone LiDAR and Structure from Motion (SfM). For this purpose, the 3D Scanner App™ dedicated to Apple devices was used.

3D DEM models were used to determine scallops length and to comparatively analyse the usefulness and limitations of using both – LiDAR and SfM methods. The obtained results allow us to conclude that the SfM models are characterised by much greater detail and precision and, thus, better reproduce the morphology of the studied surfaces of the cave walls. Using only iPhone LiDAR models often results in assigning several scallops to one, larger form. In addition, large clusters of small scallops can be misinterpreted as larger individual objects. Despite this, during the LiDAR scan, photos are taken that can allow the generate of an SfM model based on them. Therefore, the use of both measurement techniques is beneficial from the point of view of changing lighting conditions, data recording and different surface mapping potentials depending on the size and nature of the forms.

In accordance with SfM models, two generations of scallops were recognized. Both LiDAR and SfM

models allowed us to measure the scallop's length as well as determine the asymmetry of their structure. It was used for determining the paleoflow direction of Wielki Chodnik passage, which was flowing NE, and this is consistent with the modern direction of Kościeliski Potok flow. The velocity of the paleoflow ranged from 40 to 70 cm s^{-1}. Thus, the paleoflow rate was calculated at 1.93 m^3 s^{-1}, and this is similar to the values observed in Kościeliski Potok today, e.g. 1.7 m^3 s^{-1}.

The iPhone 13 Pro, as well as its later versions, is an interesting alternative to TLS and MLS scanners in cave research due to its small size, weight and relatively low price. It allows one to work in hard-to-reach parts of the cave, and the possibility of use by a larger group of users increases research opportunities. Nevertheless, the different detail of the generated SfM and LiDAR models indicates the need to analyse both models, at least in the case of cave microforms. It seems that the analysis of larger forms of relief can only be carried out using a LiDAR scanner without creating SfM models, which has already been confirmed in the literature (Luetzenburg et al. 2021).

Acknowledgements

Contributions by the authors

Together with the supervisor of the work, Dr. Andrzej Tyc, Przemysław Pluta is the author of the concept of work; he carried out the main part of the chamber work on DEM models and their comparative analysis; in addition, he developed the text part of the work.

Dawid Siemek took part in fieldwork in the cave and in the development of a numerical method for determining paleoflow directions based on scallops using models of slope and exposure indexes.

References

Baścik M., Pociask-Karteczka J., Balon J., German K., Maciejowski W., 2014. Dolina Kościeliska: śladami badaczy, artystów i wędrowców. Wydawnictwo Tatrzański Park Narodowy, Zakopane.

Bauwens S., Bartholomeus H., Calders K.,Lejeune P., 2016. Forest inventory with terrestrial LiDAR: A comparison of static and hand-held mobile laser scanning. Forests 7(6): 127. DOI: 10.3390/f7060127.

Blumberg P.N., Curl R.L., 1974. Experimental and theoretical studies of dissolution roughness. Journal of Fluid Mechanics 65(4): 735–751.

Bretz J.H., 1942. Vadose and phreatic features of limestone caverns. The Journal of Geology 50(6, Part 2): 675–811.

Buchroithner M.F., 2015. Mountaincartography 'down under'–Speleological 3D Mapping. Wiener Schriften zur Geographie und Kartographie 21(1): 93–204.

Coleman J.C., 1949. An indicator of water-flow in caves. In Proc. Univ. Bristol speleol. Soc. 6: 57–67.

Cosso T., Ferrando I., Orlando A., 2014. Surveying and mapping a cave using 3d laser scanner: the open challenge with free and open source software. The International Archives of the Photogrammetry, Remote Sensing and Spatial Information Sciences 40: 181–186. DOI: 10.5194/isprsarchives-XL-5-181-2014.

Curl R.L., 1966. Scallops and flutes. Transactions of the Cave Research Group of Great Britain 7(2): 121–160.

Curl R.L., 1974. Deducing flow velocity in cave conduits from scallops. National Speleological Society Bulletin 36(2): 1–5.

Dabove P., Grasso N., Piras M., 2019. Smartphone-based photogrammetry for the 3D modeling of a geomorphological structure. Applied Sciences 9(18): 3884. DOI: 10.3390/app9183884.

De Waele J., Gutiérrez F., 2022. Karst Hydrogeology, Geomorphology and Caves. Wiley Blackwell.

Droin A., 2021. Delineation and morphometric analysis of micro-scale karstic forms (scallops) based on structure from motion digital elevation models. Master's thesis, Karl-Franzens University of Graz.

Eitel J.U., Vierling L.A., Magney T.S., 2013. A lightweight, low cost autonomously operating terrestrial laser scanner for quantifying and monitoring ecosystem structural dynamics. Agricultural and forest meteorology 180: 86–96. DOI: 10.1016/j.agrformet.2013.05.012.

Filar F., Parczewski M., 2015. System Jaskiń Pawlikowskiego. Jaskinie 2–3: 44–45.

Gallay M., Hochmuth Z., Kaňuk J., Hofierka J., 2016. Geomorphometric analysis of cave ceiling channels mapped with 3-D terrestrial laser scanning. Hydrology and Earth System Sciences 20(5): 1827–1849. DOI: 10.5194/hess-20-1827-2016.

Gollob C., Ritter T., Kraßnitzer R., Tockner A., Nothdurft A. (2021). Measurement of forest inventory parameters with Apple iPad pro and integrated LiDAR technology. Remote Sensing 13(16): 3129. DOI: 10.3390/rs13163129.

GUGiK [Główny Urząd Geodezji i Kartografii], 2023. Geoportal Infrastrukturalny Informacji Przestrzennej. Online: www.geoportal.gov.pl – 18.02.2023.

Hercman H., 1985. Określenie prędkości i wielkości przepływu wody w korytarzach jaskiniowych na podstawie pomiarów zagłębień wirowych. Przegląd Geologiczny 33(10): 580.

James M.R., Quinton J.N., 2014. Ultra-rapid topographic surveying for complex environments: the hand-held mobile laser scanner (HMLS). Earth Surface Processes and Landforms 39(1): 138–142. DOI: 10.1002/esp.3489.

Kartini G. A. J., Gumilar I., Abidin H. Z., Yondri L., 2022. The Comparison of Different LIDAR Acquisition Software on Ipad Pro m1 2021. The International Archives of the Photogrammetry, Remote Sensing and Spatial Information Sciences 48: 117–120. DOI: 10.5194/isprs-archives-XLVIII-2-W1-2022-117-2022.

Kicińska D., Hercman H., Najdek K., 2017. Evolution of the Bystrej Valley caves (Tatra Mts, Poland) based on corrosive forms, clastic deposits and U-series speleothem dating. Annales Societatis Geologorum Poloniae 87(1): 101–119. DOI: 10.14241/asgp.2017.007.

Konsolaki A., Vassilakis E., Gouliotis L., Kontostavlos G.,Giannopoulos V., 2020. High resolution digital 3D modelling of subsurface morphological structures of Koutouki Cave, Greece. Acta Carsologica 49(2–3): 163-177. DOI: 10.3986/ac.v49i2-3.7708.

Kotański Z., 1959. Profile stratygraficzne serii wierchowej Tatr Polskich. Instytut Geologiczny, Biuletyn 139: 1–160.

Lefeld J., Gaździcki A., Iwanow A., Krajewski K., Wójcik K., 1985. Jurassic and Cretaceous lithostratigraphic units of the Tatra Mountains. Studia Geologica Polonica 84: 1–93.

Luetzenburg G., Kroon A., Bjørk A.A., 2021. Evaluation of the Apple iPhone 12 Pro LiDAR for an application in geosciences.

Scientific Reports 11(1): 22221. DOI: 10.1038/s41598-021-01763-9.

Mikita T., Krausková D., Hrůza P., Cibulka M., Patočka Z., 2022. Forest road wearing course damage assessment possibilities with different types of laser scanning methods including new iPhone LiDAR scanning apps. Forests 13(11): 1763. DOI: 10.3390/f13111763.

Mokroš M., Mikita T., Singh A., Tomaštík J., Chudá J., Wężyk P., Kuželka K., Surový P., Klimánek M., Zięba-Kulawik K.,Bobrowski R., 2021. Novel low-cost mobile mapping systems for forest inventories as terrestrial laser scanning alternatives. International Journal of Applied Earth Observation and Geoinformation 104: 102512. DOI: 10.1016/j.jag.2021.102512.

Palmer A.N., 2007. Cave Geology. Cave Books.

PIG [Państwowy Instytut Geologiczny], 2023. Jaskinie Polski. Online: jaskiniepolski.pgi.gov.pl/ – 22.03.2023.

Pukanská K., Bartoš K., Bella P., Gašinec J., Blistan P., Kovanič Ľ., 2020. Surveying and high-resolution topography of the ochtiná aragonite cave based on tls and digital photogrammetry. Applied Sciences 10(13): 4633. DOI: 10.3390/app10134633.

Rudnicki J., 1958. Geneza jaskiń system Lodowego Źródła i ich związek z rozwojem Doliny Kościeliskiej. Acta Geologica Polonica 8(2): 245–274.

Rudnicki J., 1960. Geneza zagłębień wirowych w świetle badań eksperymentalnych. Speleologia 2(1): 51–55.

Rudnicki J., 1967. Geneza i wiek jaskiń Tatr Zachodnich. Acta Geologica Polonica 17(4): 521–592.

Slabe T., 1995. Cave rocky relief and its speleogenetical significance. Založba ZRC 10. DOI: 10.3986/961618203X.

Tatsumi S., Yamaguchi K., Furuya N., 2022. ForestScanner: A mobile application for measuring and mapping trees with LiDAR-equipped iPhone and iPad. Methods in Ecology and Evolution 14(7): 1603–1609. DOI: 10.1111/2041-210X.13900.